Reprinted from Biochemistry, 1992, 31.

Phospholipase A_2 Engineering. Structural and Functional Roles of Highly Conserved Active Site Residues Tyrosine-52 and Tyrosine-73†

Cynthia M. Dupureur,‡ Bao-Zhu Yu,§ Mahendra K. Jain,*,§ Joseph P. Noel,‡,∥ Tiliang Deng,‡,⊥ Yishan Li,‡ In-Ja L. Byeon,‡ and Ming-Daw Tsai*,‡

Department of Chemistry, The Ohio State University, Columbus, Ohio 43210, and Department of Chemistry and Biochemistry, University of Delaware, Newark, Delaware 19716

Received December 4, 1991; Revised Manuscript Received May 1, 1992

ABSTRACT: Site-directed mutagenesis was used to probe the structural and functional roles of two highly conserved residues, Tyr-52 and Tyr-73, in interfacial catalysis by bovine pancreatic phospholipase A_2 (PLA2, overproduced in *Escherichia coli*). According to crystal structures, the side chains of these two active site residues form H-bonds with the carboxylate of the catalytic residue Asp-99. Replacement of either or both Tyr residues by Phe resulted in only very small changes in catalytic rates, which suggests that the hydrogen bonds are not essential for catalysis by PLA2. Substitution of either Tyr residue by nonaromatic amino acids resulted in substantial decreases in the apparent k_{cat} toward 1,2-dioctanoyl-*sn*-glycero-3-phosphocholine (DC_8PC) micelles and the v_o (turnover number at maximal substrate concentration, i.e., mole fraction = 1) toward 1,2-dimyristoyl-*sn*-glycero-3-phosphomethanol ($DC_{14}PM$) vesicles in scooting mode kinetics [Berg, O. G., Yu, B.-Z., Rogers, J., & Jain, M. K. (1991) *Biochemistry 30*, 7283–7297]. The Y52V mutant was further analyzed in detail by scooting mode kinetics: the E to E* equilibrium was examined by fluorescence; the dissociation constants of E*S, E*P, and E*I (K_S*, K_P*, and K_I*, respectively) in the presence of Ca^{2+} were measured by protection of histidine-48 modification and by difference UV spectroscopy; the Michaelis constant K_M* was calculated from initial rates of hydrolysis in the absence and presence of competitive inhibitors; and the turnover number under saturating conditions (k_{cat}, which is a theoretical value since the enzyme may not be saturated at the interface) was calculated from the v_o and K_M* values. The results indicated little perturbation in the interfacial binding step (E to E*) but ca. 10-fold increases in K_S*, K_P*, K_I*, and K_M* and a <10-fold decrease in k_{cat}. Such changes in the function of Y52V are not due to global conformational changes since the proton NMR properties of Y52V closely resemble those of wild-type PLA2; instead, it is likely to be caused by perturbed enzyme–substrate interactions at the active site. Tyr-73 appears to play an important structural role. The conformational stability of all Tyr-73 mutants decreased by 4–5 kcal/mol relative to that of the wild-type PLA2. The proton NMR properties of Y73A suggested significant conformational changes and substantially increased conformational flexibility. These detailed structural and functional analyses represent a major advancement in the structure–function study of an enzyme involved in interfacial catalysis.

Phospholipase A_2 (PLA2)[1] catalyzes the hydrolysis of the 2-acyl ester bond of 3-*sn*-phosphoglycerides. Central to the activity of this enzyme are the absolutely conserved Asp-99 and His-48, termed the catalytic dyad in the fashion of serine proteases. Hydrogen-bonded to Asp-99 are the highly conserved Tyr-52 and Tyr-73. With the exception of bee venom PLA2 (which has only one analogous tyrosine; Scott et al., 1990), the "catalytic network" (Brunie et al., 1985) formed by these four residues is invariant among all secretory phospholipases A_2 (van den Bergh et al., 1987; Verheij et al., 1981; Maraganore et al., 1987) and occupies virtually identical positions in all crystal structures (Renetseder et al., 1985; Achari et al., 1987). Additionally, it remains intact in the crystal structures of PLA2 complexes with an *sn*-2 amide analogue (Thunnissen et al., 1990) and with a transition-state analogue inhibitor (White et al., 1990; Scott et al., 1990). As depicted in Figures 1 and 2, the catalytic network is connected via a water molecule to the N-terminal region located on the surface of the enzyme, which has been suggested to be part of the "interfacial recognition site" on the basis of spectroscopic studies and the use of chemically modified or semisynthetic enzymes (Volwerk & de Haas, 1982; van Dam-Mieras et al., 1975; van Scharrenburg, et al., 1982; Dijkstra et al., 1984; Volwerk & de Haas, 1982). Speculation regarding the roles of the two tyrosines in PLA2 function has persisted (Brunie et al., 1985; Renetseder et al., 1985) ever since these structural

† This work was supported by Research Grants GM41788 (to M.-D.T.) and GM29703 (to M.K.J.) from National Institutes of Health. This is paper 7 in the series "Phospholipase A_2 Engineering". For paper 6, see Dupureur et al. (1992).

‡ The Ohio State University.

§ University of Delaware.

∥ Current address: Department of Molecular Biophysics and Biochemistry, Yale University, New Haven, CT 06511.

⊥ Current address: Deparmtent of Phamacology, School of Medicine, University of California at San Diego, La Jolla, CA 92093.

[1] Abbreviations: CD, circular dichroism; CMC, critical micelle concentration; COSY, correlated spectroscopy; 1D, one-dimensional; 2D, two-dimensional; DC_6PC, 1,2-dihexanoyl-*sn*-glycero-3-phosphocholine; DC_7PC, 1,2-diheptanoyl-*sn*-glycero-3-phosphocholine; DC_8PC, 1,2-dioctanoyl-*sn*-glycero-3-phosphocholine; $DC_{12}PG$, 1,2-dilauroyl-*sn*-glycero-3-phosphoglycerol; DC_8PM, 1,2-dioctanoyl-*sn*-glycero-3-phosphomethanol; $DC_{14}PM$, 1,2-dimyristoyl-*sn*-glycero-3-phosphomethanol; deoxy-LPC, 1-hexadecylpropanediol-3-phosphocholine; DTPC, 1,2-ditetradecyl-*sn*-glycero-3-phosphocholine; DTPM, 1,2-ditetradecyl-*sn*-glycero-3-phosphomethanol; EDTA, ethylenediaminetetraacetate; GdnHCl, guanidine hydrochloride; HDNS, dansylated hexadecylphosphoethanolamine; MJ33, 1-hexadecyl-3-trifluoroethyl-*sn*-glycero-2-phosphomethanol; NOE, nuclear Overhauser effect; NOESY, nuclear Overhauser enhancement spectroscopy; PLA2, phospholipase A_2; Tris, 2-amino-2-(hydroxymethyl)-1,3-propanediol; WT, wild-type.

0006-2960/92/0431-6402$03.00/0

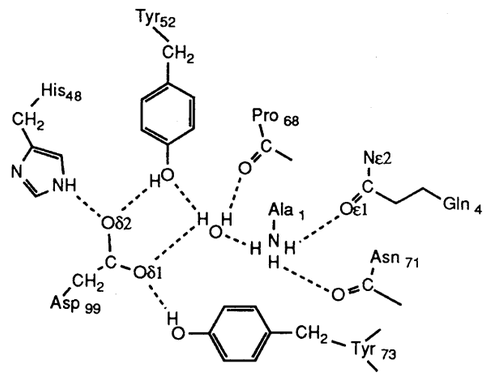

FIGURE 1: The H-bonding network connecting the active site residues and the interfacial site at the N-terminus (Dijkstra et al., 1983).

features were first elucidated. Do Tyr-52 and Tyr-73 provide critical support to the Asp-99···His-48 catalytic dyad? Are the contributions of these two residues vital to the hydrogen-bonding network and thus to interfacial catalysis?

While contributions of the N-terminal amino acid residues to the network have been probed by semisynthetic methods, Tyr-52 and Tyr-73 are much less accessible by chemical means. Indeed, in an extensive chemical modification study of tyrosines in PLA2, Tyr-52 and Tyr-73 were among the conserved tyrosines unmodified by tetranitromethane (Meyer et al., 1979). Both the cloistered location and the structural features surrounding these two residues make them excellent candidates for site-directed mutagenesis studies. Therefore, in an effort to understand the roles of these two tyrosines both in the network and in interfacial catalysis, we report the structural and functional roles of Tyr-52 and Tyr-73. Interfacial catalysis by specific Y52/Y73 mutant enzymes was characterized through the use of monomeric, micellar, and bilayer forms of substrates. Additional methods were employed to obtain the catalytic and binding parameters[2] in the scooting mode and to distinguish the binding of the enzyme to the interface from the binding of the substrate monomers to the active site of PLA2 bound at the interface (Berg et al., 1991). These functional studies were supported (and complemented) by analyses of conformation and conformational stability.

The results show that the H-bonds between Y52/Y73 and the carboxylate of Asp-99 are not essential to catalysis, but the aromatic side chains of both are required for optimal activity. Tyr-73 has been shown to play important structural roles whereas Tyr-52 has been shown to play significant functional roles. A preliminary account of part of the results has been published (Dupureur et al., 1990). Related results for porcine PLA2 have also been reported to Kuipers et al. (1990). These two earlier papers reported only conventional micellar and monomeric kinetic data, but the results are generally consistent between porcine and bovine PLA2.

Materials and Methods

Materials and Routine Procedures. Oligonucleotides were obtained from the Biochemical Instrument Center at the Ohio State University. The following lipids used in this study were prepared as described previously: DTPM (Jain et al., 1986); $DC_{14}PM$ (Jain & Gelb, 1991); HDNS (Jain & Vaz, 1987); MJ33 (Jain et al., 1991d). All other phospholipid substrates were purchased from Avanti Polar Lipids (Birmingham, AL). Ultrapure guanidine hydrochloride was purchased from ICN Biochemicals. Other chemicals and biochemicals were of the highest quality available commercially. CD spectra were recorded on a JASCO J-500C spectropolarimeter using a thermostated quartz microcell and processed using DP-500/AT system (version 1.29) software.

Construction and Purification of Mutant Enzymes. Site-directed mutants were constructed using an Amersham mutagenesis kit according to the manual provided by the manufacturer. The position 52 mutant enzymes were constructed from the oligonucleotides 5′ GC TTG TTT CTT GCA ATT ATC ATG 3′ (Y52K) and 5′ GC TTG TTT A(G/A)(C/A) GCA ATT ATC ATG 3′. Confirmed mutations with the second oligonucleotide were AAA (Y52F) and AAC (Y52V). Mutant enzymes at position 73 were constructed with 5′ GCT GTA AGA GAA GTT ATT TG 3′ (Y73F), 5′ GCT GTA AGA CTT GTT ATT TG 3′ (Y73K), and 5′ GCT GTA AGA GG(C/A) GTT ATT TG 3′ (Y73A and Y73S, respectively).

Recombinant PLA2 was isolated from the *Escherichia coli* expression host, BL21 (DE3)[pLysS], carrying the pTOpropla2 plasmid (Deng et al., 1990). All PLA2 enzymes were purified as described elsewhere (Noel et al., 1991) with the following modifications. Following lysis and refolding, the pH

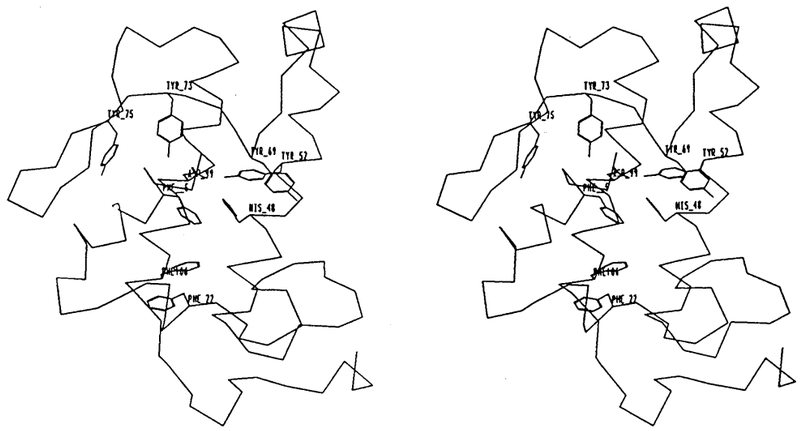

FIGURE 2: Stereoview of the α-carbon traces of bovine pancreatic PLA2 from the 1.8-Å crystal structure (Noel et al., 1991), with the side chains of pertinent residues highlighted. The designation of helices A–E used in the text is according to Dijkstra et al. (1978): A (1–13), B (19–22), C (40–58), D (59–64), and E (90–108).

of the protein solution was lowered to 4.8 with glacial acetic acid and the solid was removed by centrifugation. The supernatant was dialyzed overnight against distilled water at 4 °C and subsequently loaded onto a small Sepharose-S column. This served to both concentrate the protein and remove many impurities prior to trypsin digestion. Activation and anion-exchange chromatography were conducted as previously described.

Kinetic Analysis. Activities toward micellar and monomeric PC substrates were conducted at 45 °C on a Radiometer RTSS titration system as previously described (Noel et al., 1991). The apparent V_{max} and K_m were determined from Eadie–Hofstee plots (Atkins & Nimmo, 1975) of v vs $v/[S]$ by use of linear regression analyses. The apparent k_{cat} was calculated from V_{max} on the basis of a molecular weight of 13 500. The specific activity toward monomeric DC_6PC was assayed at 5 mM. The negatively charged mixed micelles of $DC_{12}PG$ (at 5 mM) and sodium deoxycholate (at 15 mM) were prepared and assays were conducted as described previously (Noel et al., 1991). Kinetic analysis of PLA2 in the scooting mode on $DC_{14}PM$ vesicles was carried out as described previously using a pH-stat method under first-order (Jain et al., 1986; Jain & Gelb, 1991; Berg et al., 1991) or zero-order conditions (Berg et al., 1991; Jain et al., 1991c). The data reported for DC_8PM are the initial rates with 1 mM substrate at 23 °C. Since the substrate concentration dependence of the initial rate of hydrolysis of this substrate does not exhibit anomalous behavior at the CMC, presumably because pancreatic PLA2s form premicellar aggregates with anionic amphiphiles, the enzyme should be fully bound to the interface in this system (Jain & Rogers, 1989).

Dissociation Constants. (*a*) *Protection Methods.* The equilibrium dissociation constants for the dissociation of ligands (calcium, inhibitors, products, and the ether analogue DTPM) bound to the active site of PLA2 at the interface or in the aqueous phase were determined by monitoring the rate of alkylation of His-48 by 2-bromo-4′-nitroacetophenone as detailed elsewhere (Jain et al., 1991a). Briefly, PLA2 (30 μM) was incubated at 22 °C in 50 mM cacodylate buffer, pH 7.3, in the presence of 2 mM deoxy-LPC, 0.8 mM 2-bromo-4-nitroacetophenone, and the appropriate ligands. At various time intervals, an aliquot containing typically 0.1–100 pmol of the enzyme was diluted into an appropriate assay mixture (Jain et al., 1991c; Niewenhuizen et al., 1974; Radvanyi et al., 1989). The nonlinear regression of the plot of the residual PLA2 activity as a function of time provided the rate constant for inactivation. The equilibrium dissociation constant under a given set of conditions was calculated from the Scrutton–Utter equation described elsewhere (Jain et al., 1991a).

(*b*) *Spectroscopic Methods.* Binding of PLA2 to DTPM vesicles was studied by monitoring the resonance energy transfer from the tryptophan residue (Trp-3) on the PLA2 (excitation at 285 nm) to the dansyl probe on the HDNS present in the vesicles or by directly (excitation at 347 nm) monitoring the fluorescence emission of the HDNS without energy transfer (Jain & Vaz, 1987). All measurements were carried out on an SLM 4800S spectrofluorometer. Solutions contained vesicles of DTPM (0.2 mg) and HDNS (4 μg) in 1.5 mL of 10 mM Tris-HCl, 0.5 mM $CaCl_2$, pH 8.0. The fluorescence of the solution was monitored following addition of increasing amounts of the enzyme. Emission was monitored at 495 nm and the slit width was 4 nm for both emission and excitation.

The absorbance of PLA2 in the 230–340-nm region was monitored by a UV–visible spectrophotometer (Hewlett-Packard Model 8452) equipped with a diode array detector. The standard software package from this spectrophotometer allowed manipulations that were necessary for obtaining the difference spectra. The resolution of the spectra was 2 nm, and therefore the peaks in the difference spectra appear sharper than those reported by Hille et al. (1983). Under certain conditions, we noticed minor contributions from scattering by micelles. In such cases, the experiments were designed such that these contributions could be subtracted. Typically, the PLA2 concentration was 35 μM in 20 mM Tris-HCl and 5 mM $CaCl_2$ at pH 8.0. The first addition was usually of the neutral diluent (deoxy-LPC), and then appropriate amounts of ligands were added in small volumes such that the overall dilution was less that 5%. The spectra were corrected for such dilution before subtractions were made for obtaining the difference spectra.

GdnHCl-Induced Denaturation and Circular Dichroism Spectroscopy. Enzyme samples for GdnHCl denaturation were prepared by dissolving the lyophilized enzyme into 10 mM sodium borate, 0.1 mM EDTA, pH 8.0, to a concentration of approximately 3 mg/mL as determined spectrophotometrically (Volwerk & de Haas, 1982). A stock solution of GdnHCl near 8.5 M was prepared in the same buffer and the exact concentration was determined by refractive index (Nozaki, 1972). Both solutions, along with the buffer, were used to prepare 15–20 different solutions at various concentrations of GdnHCl; the concentration of enzyme was always near 0.05 mg/mL. Samples were incubated at 30 °C for at least 10 min prior to measurement. Typically five scans were signal averaged to produce a CD spectrum from 250 to 200 nm. For each sample, a background spectrum of a solution of the appropriate concentration of GdnHCl in borate was collected and subtracted from the sample spectrum. The resulting observed ellipticity at 222 nm was recorded as a measure of the degree of structure present in the enzyme at each concentration of GdnHCl (Greenfield & Fasman 1969).

NMR Analysis. The enzyme sample was dissolved in D_2O (99.9 atom % D, MSD Isotopes), and salts were added with stock solutions of $CaCl_2$ and NaCl, both in D_2O. The solution was kept at room temperature for 1 h to allow for deuterium exchange and then lyophilized. After the exchange process was repeated, the sample was dissolved in 0.4–0.5 mL of D_2O (99.96 atom % D, Cambridge Isotope) and the pH* (uncorrected pH from pH meter reading) was adjusted to 4.0–4.1 with DCl and NaOD stock solutions (MSD Isotopes). The final NMR samples contained 1.0 mM enzyme, 50 mM $CaCl_2$, and 300 mM NaCl. Proton NMR spectra were recorded on a Bruker AM 500 spectrometer at 37 °C, unless otherwise specified. Chemical shifts are referenced to internal sodium 3-trimethylsilyl[2,2,3,3-D_4]propionate (TMSP).

Results

Catalytic Rates. The activities of the mutant enzymes were measured in five different assay systems: $DC_{14}PM$ vesicles, DC_8PC micelles, DC_6PC monomers, DC_8PM micelles, and $DC_{12}PG$/deoxycholate mixed micelles. The results are listed in Table I, and the significance of each assay is briefly ex-

[2] Definition of kinetic parameters *at the interface*: K_I*, dissociation constant of inhibitor; K_M*, Michaelis constant; K_P*, dissociation constant of product; K_S*, dissociation constant of substrate; k_{cat}, turnover number at saturating substrate concentration; N_S, the number of phospholipids in the outer molayer of the vesicle; $N_S k_i$, apparent second-order rate constant; v_o, turnover number at $X_S = 1$; X_I, mole fraction of inhibitor; X_S, mole fraction of substrate. It should be noted that notations K_I*, K_M*, K_P*, and K_S* correspond to K_i, K_{MS}, K_P, and K_S, respectively, used previously (Berg et al., 1991). The revised notations will be used in our future work.

Table I: Summary of Kinetic Data for WT and All Mutants

enzymes	$DC_{14}PM$ vesicle v_o (s^{-1})	DC_8PC micelle $k_{cat,app}$ (s^{-1})	DC_8PC micelle $K_{m,app}$ (mM)	DC_6PC monomer[a]	DC_8PM micelle[b]	$DC_{12}PG$ micelle[a,c]
WT	330	675	1.4	1.2	830	440
Y52F	330	265	1.4	0.90	2820	175
Y73F	560	580	2.0	0.47	1700	98
Y52F/Y73F	380	205	2.8	0.14	2350	164
Y52V	11	1.0	0.7	0.07	90	18
Y52K		5.1	5.1	0.30		
Y73S	40	1.7	0.9	0.09	670	20
Y73A	60	4.0	1.8	0.07	330	34
Y73K	30	0.9	1.5	0.02	130	

[a] Specific activity (s^{-1}) at 5 mM substrates. [b] Specific activity (s^{-1}) at 1 mM substrates. [c] Mixed micelles with 3 equivalents of sodium deoxycholate.

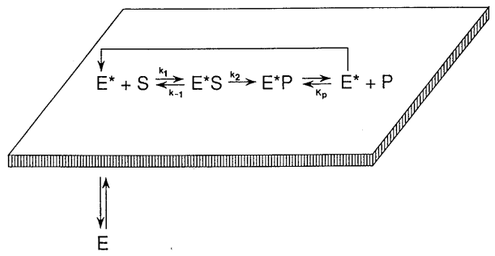

FIGURE 3: A kinetic scheme to account for key features of interfacial catalysis by PLA2. The species (E*, enzyme, S, substrate, P, product) shown in the box plane are in or bound to the interface. The enzyme in the aqueous phase is shown as E. During catalysis in the scooting mode, all the enzyme remains in the interface. See Berg et al. (1991) for complete elaboration of this scheme.

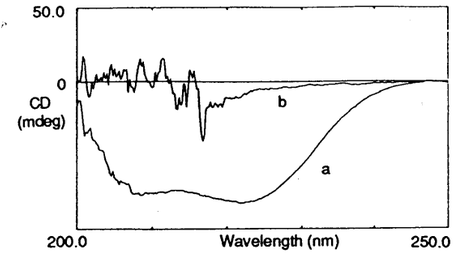

FIGURE 4: CD spectra of WT PLA2 in the native form (curve a) and the fully denatured form (curve b). Conditions: (a) 10 mM sodium borate, 0.1 mM EDTA, 0.05 mg/mL PLA2, pH 8.0; (b) in the presence of 8.5 M GdnHCl.

plained as follows. The data reported for DC_6PC monomers, DC_8PM micelles, and $DC_{12}PG$/deoxycholate mixed micelles are only specific activities (turnover number per enzyme molecule at a fixed substrate concentration) and will not be seriously interpreted. In the DC_8PC micelle assay, k_{cat} and K_m were derived with the assumption that classical Michaelis–Menten kinetics are obeyed. Since the assumption may not be valid as explained in the Discussion, k_{cat} and K_m should be considered as apparent values ($k_{cat,app}$ and $K_{m,app}$, respectively). The $DC_{14}PM$ vesicle system is the scooting mode assay developed by Jain and co-workers (Jain & Berg, 1989; Jain et al., 1991), which permits measurements of kinetic constants exclusively at the interface, without being complicated by the E to E* equilibrium shown in Figure 3. The v_o values listed in Table I are defined by (Jain et al., 1991a)

$$v_o = k_{cat}X_S/(K_M^* + X_S) \quad (1)$$

This equation is analogous to the Michaelis–Menten equation, except that the substrate concentration X_S (therefore also K_M^*, the Michaelis constant in the scooting mode) is represented by mole fractions. The initial velocity v_o is actually the turnover number at the concentration "seen" by the enzyme bound to the interface. It can be considered as the turnover number at the maximal substrate concentration since the actual mole fraction cannot exceed 1 ($X_S = 1$ for $DC_{14}PM$ vesicles), but it is not necessarily a saturating concentration for the formation of the E*S complex.

The results from all the assay methods indicate that substitution of Tyr-52 and/or Tyr-73 by phenylalanine resulted in only small changes in the activity, which suggests that the hydrogen bonding between these two tyrosine residues and the carboxylate of Asp-99 is not essential to catalysis. However, replacement of Tyr-52 or Tyr-73 by nonaromatic amino acids, including some which can function as H-bond donors, resulted in substantial decreases in the $k_{cat,app}$ toward DC_8PC micelles (130–750-fold) and smaller changes in the v_o toward $DC_{14}PM$ vesicles (<30-fold). The possible reasons for the quantitative variations in the different assay systems will be discussed later. However, the results clearly suggest that the aromatic rings of Tyr-52 and Tyr-73 are important to the function and/or structure of PLA2.

Structural Properties. The lack of functional roles for the phenolic hydroxyl groups of Tyr-52 and Tyr-73 raises two structural questions: (i) whether the roles of the phenolic hydroxyls have been replaced by water molecules or other residues at the active site; and (ii) whether the two phenolic hydroxyls contribute to conformational stability. The high-resolution X-ray structure of the Y52F/Y73F double mutants does not reveal any additional water around the two residues (C. Sekharudu, B. Ramakrishnan, B. Huang, R.-T. Jiang, C. M. Dupureur, M. Sundaralingam, and M.-D. Tsai, unpublished results). The second question was addressed by determining the free energy of denaturation. For nonaromatic mutants, it is important to determine if the decreased activity is caused by changes in the global conformation of the enzyme before the perturbation in the kinetic data can be interpreted. This problem was addressed by 1D and 2D proton NMR analysis.

(*a*) *Conformational Stability.* Since this is the first systematic study of this type for bovine PLA2 and its mutant enzymes, we experimented with a number of denaturants and observation methods in an effort to select the most sensitive approach. Chemical denaturation provides the most complete and reversible means for unfolding proteins (Pace, 1975). GdnHCl is among the strongest of reversible chemical denaturants (Pace & Marshall, 1980) and as such is especially suited for application to the rugged PLA2. Circular dichroism spectroscopy is quite sensitive to changes in the secondary structure of proteins, particularly with those high in helical content like PLA2 (Scanu et al., 1969; Dufton et al., 1983) and thus affords an advantage over other forms of spectroscopyl(Greenfield & Fasman, 1969). Figure 4 shows the CD

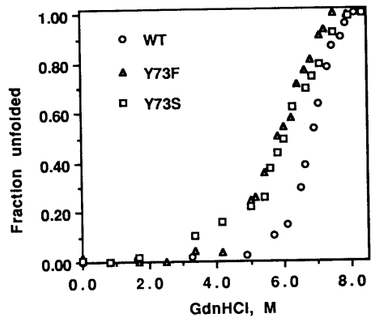

FIGURE 5: Denaturation curves. Conditions are as described in Figure 4. Fraction unfolded = $1 - (\theta_i - \theta_D)/(\theta_N - \theta_D)$, where θ_N and θ_D are the observed ellipticities at 222 nm for native and denatured states, respectively, and θ_i is the observed ellipticity at a given GdnHCl concentration.

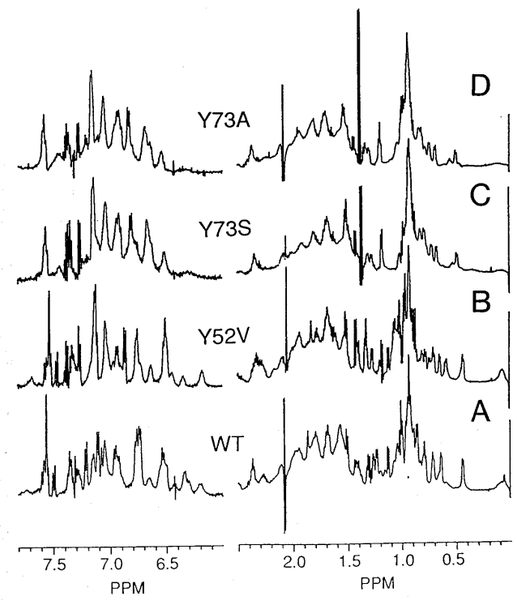

FIGURE 6: One-dimensional proton NMR spectra of WT (A), Y52V (B), Y73S (C), and Y73A (D). Sample conditions are described in Materials and Methods.

spectra of native and fully denatured WT PLA2 (there are no significant differences for the mutant enzymes). Figure 5 shows the denaturation curves of WT and two mutants. These curves display behavior consistent with an apparent two-state folding mechanism, which were then analyzed by the standard equation

$$\Delta G_d = \Delta G_d^{H_2O} - m[\text{GdnHCl}] \quad (2)$$

where ΔG_d is the Gibbs free energy change at various concentrations of GdnHCl, $\Delta G_d^{H_2O}$ is that at zero concentration of GdnHCl, and m is a constant related to the susceptibility of the enzyme toward denaturation by the denaturant.

The $\Delta G_d^{H_2O}$ and m values, along with the midpoint of the denaturation curve ($D_{1/2}$), are listed in Table II. Substitution of Tyr-73 by Phe, Ser, Lys, or Ala lowered the $\Delta G_d^{H_2O}$ by 4–5 kcal/mol, suggesting that Tyr-73 contributes significantly to the conformational stability of PLA2. The changes for the Tyr-52 mutants, particularly Y52V, are much less pronounced.

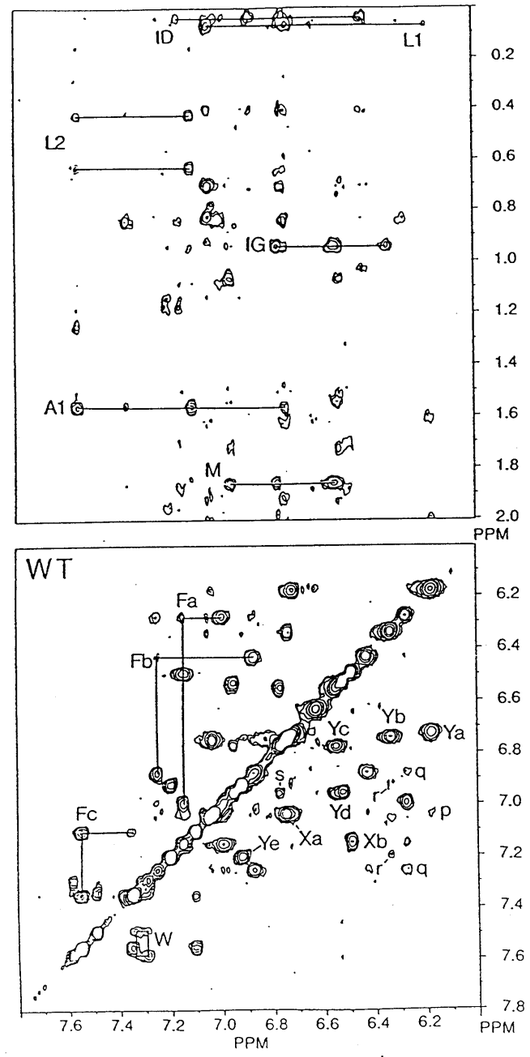

FIGURE 7: The phase-sensitive NOESY spectrum of WT, with a 200-ms mixing time, at 37 °C. The identified spin systems are labeled as follows: 5 of the 7 tyrosines (Ya–Ye), 3 of the 4 phenylalanines (Fa–Fc), and the single tryptophan (W). Two of the unidentified spin systems are labeled as Xa and Xb. The NOE cross-peaks p, q, r, and s arise from Ya/Xa, Fa/Fb, Yb/Ye, and Yc/Yd, respectively.

(*b*) *Proton NMR Properties.* Analysis was accomplished by comparing the chemical shift changes of the aromatic spin systems, as well as the interresidue NOE cross-peaks. Large changes in these two properties suggest global conformational changes and prompt caution in correlating results with functional roles of the mutated residues. On the other hand, if the changes in chemical shifts and NOESY cross-peaks are small and/or localized, the changes in the functional properties of the mutants are more likely to be caused by the *site-specific* changes in the structure.

For each of the tyrosine residues, we characterized the NMR properties of representative aliphatically-substituted mutants. Figure 6 shows the 1D spectra of WT and these mutants. There are some differences in the 1D spectra, which were further characterized by 2D experiments. The NOESY spectra of the aromatic region for WT, Y52V, and Y73A are

Table II: Free Energy of Denaturation Induced by GdnHCl[a]

enzymes	$\Delta G_d^{H_2O}$ (kcal/mol)	$D_{1/2}$ (M)	m [kcal/(mol·M)]
WT PLA2	9.5	6.9	1.47
pro-PLA2	11.0 (+1.5)	6.7	1.65
Y52F	7.7 (−1.8)	6.3	1.24
Y52V	9.9 (+0.4)	6.9	1.45
Y52K	6.8 (−2.7)	6.0	1.14
Y52F/Y73F	4.1 (−5.4)	5.2	0.79
Y73F	5.3 (−4.2)	5.9	0.90
Y73S	4.6 (−4.9)	6.0	0.77
Y73A	4.8 (−4.7)	5.8	0.83
Y73K	5.3 (−4.2)	5.9	0.90

[a] Numbers of parentheses are differences between mutants and WT, i.e., $\Delta\Delta G_d^{H_2O}$.

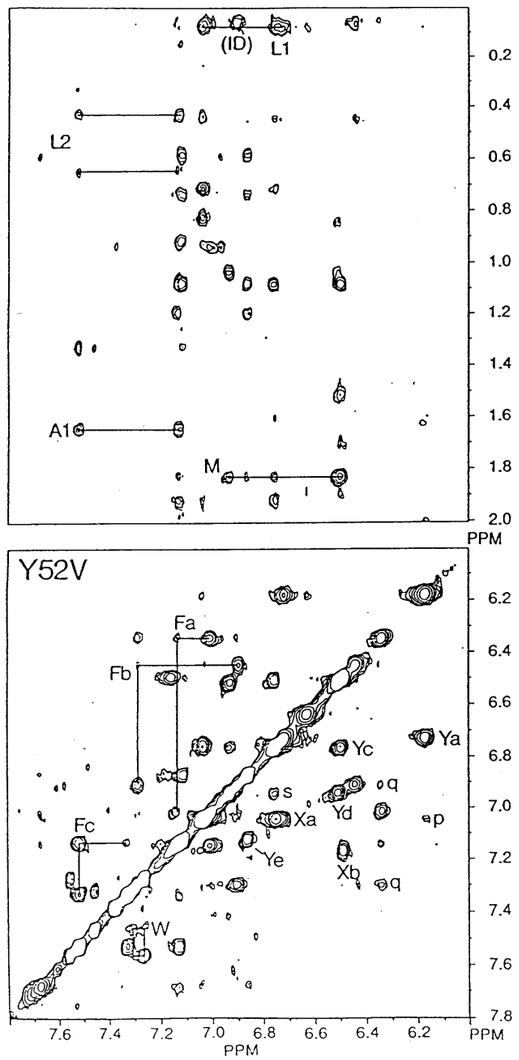

FIGURE 8: The phase-sensitive NOESY spectrum of Y52V with a 200-ms mixing time at 37 °C. The pattern is very similar to that of WT, except that the spin system Yb and the NOE cross-peaks r (between Yb and Ye) disappear.

shown in Figures 7–9, which indicate striking similarity between WT and Y52V but substantial differences between WT and Y73A. The main differences between the NOESY spectra

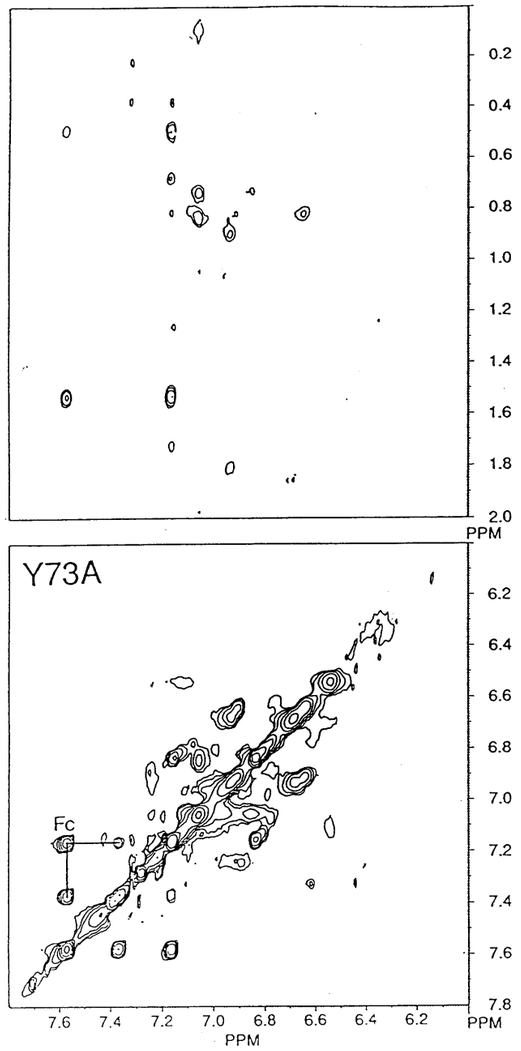

FIGURE 9: The phase-sensitive NOESY spectrum of Y73A with a 200-ms mixing time at 37 °C. No interresidue aromatic–aromatic NOEs are detectable; there are considerably fewer aliphatic–aromatic NOEs.

of WT and Y52V are that Yb has disappeared, Ye is shifted substantially, and the NOE cross-peaks between these two tyrosine residues (peaks r) have disappeared in Y52V. These features led to the assignment of Tyr-52 to Yb and the tentative assignment of Tyr-69 to Ye since Tyr-69 is the tyrosine residue closest to Tyr-52 according to the crystal structure shown in Figure 2. Although the proton NMR resonances of *porcine* PLA2 have been completely assigned (Dekker et al., 1991a), only some spin systems have been identified for *bovine* PLA2 (Fisher et al., 1989). Our assignments on the basis of the differences between WT and Y52V agree with theirs.

For WT and Y52V, the chemical shifts of the aromatic rings have been identified from the COSY spectra (not shown) and NOESY spectra and are listed in Table III. Only five resonances (underlined) differ by >0.03 ppm between WT and Y52V, and the largest difference is only 0.09 ppm. Thus it can be concluded that the conformation of Y52V is little

Table III: Chemical Shifts of the Assigned Spin Systems for WT and Y52V[a]

spin system[b]	possible assignment[c]	WT			Y52V		
Fa	(F5)	6.28	7.00	7.15	6.34	7.00	7.14
Fb	F106	6.43	6.88	7.26	6.44	6.90	7.29
Fc	F94	7.10	7.35	7.55	7.12	7.33	7.52
Ya	Y111	6.18	6.72		6.17	6.72	
Yb	Y52	6.34	6.74				
Yc	Y73	6.55	6.78		6.50	6.75	
Yd	Y75	6.52	6.95		6.51	6.94	
Ye	Y69	6.92	7.20		6.86	7.11	
W	W3	7.30	7.34	7.48	7.27	7.31	7.45
		7.58			7.54		
Xa	(F22)	6.75	7.04		6.75	7.03	
Xb	(Y28)	6.49	7.15		6.49	7.16	
ID	(I9)	0.05			0.06		
L1	(L41)	0.07			0.09		
L2	L58	0.63	0.44		0.64	0.43	
IG	I95	0.94			ni[b]		
A1	(A55)	1.56			1.70		
M	(M8)	1.86			1.84		

[a] The underlined are resonances which differ by >0.03 ppm between WT and Y52V. [b] Designation of spin systems is according to that in Fisher et al. (1989). [c] Assignments of residues are based on the comparisons between WT and Y52V as described in the text and between WT and F22 and F106 mutants (C. M. Dupureur, unpublished results). The results agree with those of Fisher et al. (1989) obtained under slightly different conditions (pH* 5.2).

perturbed. On the other hand, the conformation of Y73A appears to have been substantially perturbed judging from the 2D NOESY and COSY spectra, and it was not possible to identify all of the corresponding spin systems for Y73A. The NMR properties of Y73S are very nearly the same (Dupureur et al., 1992). These results are consistent with the observation that Y52V is least perturbed and Y73A and Y73S are greatly perturbed in conformational stability, as described in the previous section.

The lack of interresidue NOEs in the NOESY spectrum of Y73A led us to suspect whether this mutant retains the integrity of the PLA2 structure. The answer is positive since the CD spectrum of Y73A (not shown) is almost identical to that of WT, and the mutant still retains substantial activity as shown in Table I. It is also unlikely that Y73A consists of a mixture of active and denatured proteins since the N_S values determined from the same amount of Y73A and WT are the same within experimental errors (see a later section). The lack of NOEs, therefore, reflects flexibility in conformation, which again agrees with the large decrease in the $\Delta G_d^{H_2O}$ of this mutant.

Equilibrium Dissociation Constants of WT and Y52V. Since Y52V showed the largest decrease in turnover numbers and very small perturbations in structure, it was chosen for detailed analysis of kinetic and equilibrium constants. The purpose is to pinpoint the specific step(s) which differs between Y52V and WT. Most of the measurements have been performed according to the recent reports for *porcine* pancreatic PLA2 (Berg et al., 1991; Jain et al., 1991a). Since our system is *bovine* pancreatic PLA2, it was necessary to measure the constants for both WT and Y52V. The specific experiments are explained as follows.

(*a*) *The E to E* Step.* As shown in Figure 10, the relative fluorescence of HDNS in DTPM vesicles increases with the amount of WT or Y52V. As shown elsewhere for porcine pancreatic PLA2 (Jain & Vaz, 1987), such an increase in the fluorescence intensity is due to the resonance energy transfer from the tryptophan donor on the protein (Trp-3) to the dansyl acceptor localized at the bilayer interface; the change is not observed when the protein is added to a suspension of HDNS alone. As was the case with the porcine enzyme, the maximal change is observed when the lipid to enzyme mole ratio approaches 40 for both Y52V and WT. Since the initial rising

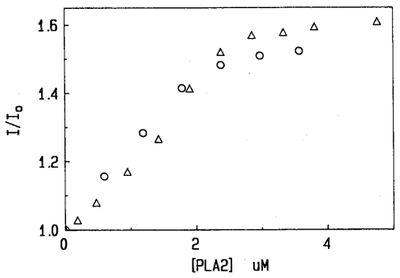

FIGURE 10: Dependence of the relative fluorescence emission intensity at 495 nm on the concentration of WT (circles) and Y52V (triangles) PLA2. The reaction mixture contained DTPM (0.2 mM) and HDNS (0.004 mM) in 10 mM Tris–chloride and 0.5 mM $CaCl_2$ at pH 8.0.

phase is linear and steep in both cases, it is not possible to compute the equilibrium dissociation constant for the protein bound to the interface (Jain et al., 1982). However, in the case of porcine PLA2, other experiments (Jain et al., 1982, 1986a; Jain & Vaz, 1987) suggested that the apparent dissociation constant is <1 μM when such binding curves are observed, i.e., virtually all molecules of both Y52V and WT were located at the interface under the conditions used for the kinetic measurements with $DC_{14}PM$ vesicles. This conclusion was further confirmed by the N_S values determined under catalytic conditions described in a later section.

(*b*) *Interfacial Binding of Ligands to E* by the Protection Method.* The equilibrium dissociation constants for the binding of a variety of ligands to PLA2 bound to the interface of deoxy-LPC are summarized in Table IV. As described by Jain et al. (1991a), these parameters were obtained from the halftimes for the alkylation of His-48 at the catalytic site of PLA2 at the interface of the neutral diluent, deoxy-LPC, in the presence and in the absence of the ligand. The halftimes of inactivation for the alkylation of WT and Y52V in the aqueous phase (without Ca^{2+}) were approximately the same (first row in Table IV), which suggested that the accessibility of the His-48 at the catalytic site was not significantly altered in this mutant. The second and third rows in Table IV indicate that the mutants behave similarly to WT in the affinity for calcium in the aqueous phase (E·Ca) and in the interface of deoxy-LPC micelles (E*·Ca). The next two rows show that

Table IV: Equilibrium Dissociation Constants of WT and Mutant Enzymes[a]

complexes	parameter	unit	WT	Y52V	Y52F	Y73S
E	inactivation halftime	min	1.5	1.3	0.4	7.7
E·Ca	K_{Ca}	mM	0.31	0.34	0.13	0.77
E*·Ca	K_{Ca}*	mM	0.12	0.1	0.22	0.33
E*·deoxy-LPC		mole frac	>1	>3	>1	>1
E*Ca·deoxy-LPC		mole frac	>1	>1	>2	>1
E*·DTPM		mole frac	0.05	–	–	–
E*Ca·DTPM	K_S*	mole frac	0.02	0.2	0.04	>0.2
E*Ca·Prod ($DC_{14}PM$)	K_P*	mole frac	0.03	0.25	0.04	>0.2
E*Ca·DTPC	K_S*	mole frac	>0.1	>0.5	>0.1	>0.2
E*Ca·MJ33	K_I*	mole frac	0.01	>0.2	>0.02	>0.1
E*Ca·MJ33[b]	K_I*	mole frac	0.01	0.22		

[a] Determined by the protection method. The dissociation constant is for dissociation of the last species in the complex shown after the dot. [b] Determined by spectroscopic characterization.

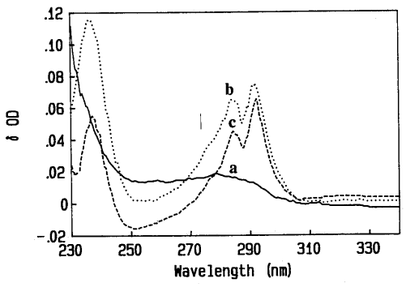

FIGURE 11: UV difference spectra for WT (0.035 mM) obtained by adding (a) 1.9 mM deoxy-LPC, (b) 1.9 mM deoxy-LPC and 0.06 mM MJ33, and (c) 0.2 mM MJ33 only. The buffer contained 50 mM Tris–chloride and 5 mM $CaCl_2$, pH 8.0.

the affinities for deoxy-LPC in the absence of calcium (E*·deoxy-LPC) and in the presence of calcium (E*Ca·deoxy-LPC) are weak for both WT and the mutants, suggesting that deoxy-LPC is a good neutral diluent for both WT and the mutants. These results justify the use of this technique to compare the relative binding affinities of WT and mutants to substrate (analogues) and inhibitors.

The data in rows 7 and 8 show that the dissociation constants for the substrate analogue DTPM and the products of hydrolysis of $DC_{14}PM$ are higher by an order of magnitude for Y52V than those for WT and Y52F. These results suggest that *both the E* to E*S equilibrium and the E*P to E* equilibrium have been shifted toward E* by a factor of ca. 10.* The same is true for the E* to E*I equilibrium, since the dissociation constant for a competitive inhibitor MJ33, a 1,3-dialkyl-*sn*-glycero-2-phosphomethanol (Jain et al., 1991d), is also higher for Y52V by the same order of magnitude (second to last row in Table IV).

(*c*) *Interfacial Binding of Ligands to E* by Spectroscopic Characterization.* The difference in K_I* values between WT and Y52V was further demonstrated by spectroscopic methods for the competitive inhibitor MJ33 (Jain et al., 1991d). As shown by the UV absorbance difference spectra for WT PLA2 in Figure 11, addition of deoxy-LPC micelles (>55-fold relative to the enzyme) induces relatively small and featureless changes in the 280–300-nm region (spectrum a) reflecting the E to E* transition. Further addition of the competitive inhibitor MJ33 (2-fold relative to the enzyme) induced characteristic changes in this region (spectrum b), reflecting the E* to E*I transition. These two spectra clearly differentiate the two processes. When the neutral diluent is omitted, MJ33 can induce the same changes, but to a smaller extent since even at a higher concentration (6-fold) the MJ33 micelle is insufficient to convert all E to E* (spectrum c). Qualitatively similar results have been observed for Y52V (spectra not shown). However,

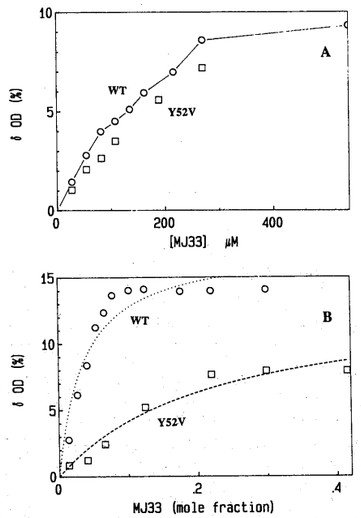

FIGURE 12: Intensity at 292 nm in the difference spectra of WT and Y52V, as a function of the concentration of MJ33, in the absence (A) and the presence (B) of 1.9 mM deoxy-LPC. Notice that the concentration is millimolar in panel A but in mole fractions in panel B. The smooth lines in panel B were the theoretical curves for a rectangular hyperbola from which the values of K_I* were obtained. Other conditions are as in the legend of Figure 11.

the affinity toward MJ33 is different between WT and Y52V, as shown by the concentration dependence curves in Figure 12. In Figure 12, the intensities at 292 nm in the difference spectra are plotted against the concentration of MJ33 in the absence (panel A) and presence (panel B) of deoxy-LPC. In panel A, both WT and Y52V showed linear increases which level off at ca. 10% difference. The experiment for panel A did not resolve the difference between WT and Y52V since the [inhibitor]/[diluent] ratio is 1 in both cases (i.e., MJ33 serves as the inhibitor as well as the diluent). In panel B, the *x*-axis is the "mole fraction" of MJ33 in the mixed micelles with the neutral diluent deoxy-LPC, and the curves are approximately hyperbolic. From these plots, the maximal change in the absorbance at 292 nm was calculated to be similar between WT (16%) and Y52V (13%). However, the mole fraction of MJ33 required for 50% increase in the absorbance was 0.01 for WT versus 0.22 for Y52V. These values are in good agreement with the corresponding values obtained by the protection method.

Equilibrium dissociation constants have also been determined for Y52F and Y73S. The data for Y52F are similar to those of WT. The data for Y73S are not interpreted because of the structural perturbations in this mutant (Dupureur

Table V: Catalytic Parameters for the Hydrolysis of $DC_{14}PM$ by WT and Y52V

parameter	unit	WT	Y52V
v_o	s^{-1}	330	11
$X_I(50)$ for MJ33	mole frac	0.025	0.22
K_M*	mole frac	0.65	>3.5
$N_S k_i$	s^{-1}	30	2.5
k_{cat}/K_M*	s^{-1}	1030	12.5
k_{cat}	s^{-1}	670	>50

et al., 1992) and the related mutant Y73A described in this paper. The difference UV spectrum of Y73S induced by MJ33 in deoxy-LPC (not shown) is noticeably different from that of WT and Y52V (Figure 11b).

Catalytic Parameters of WT and Y52V in the Scooting Mode. In this section, we present the kinetic parameters determined under catalytic conditions using $DC_{14}PM$ vesicles as substrates. The results are summarized in Table V and explained as follows.

(*a*) *K_M*, the Michaelis Constant at the Interface in the Scooting Mode.* This was calculated from initial rates of hydrolysis of $DC_{14}PM$ in the absence and presence of the competitive inhibitor MJ33 [$(v_o)^0$ and $(v_o)^I$, respectively] according to the following equation (Berg et al., 1991; Jain et al., 1991a):

$$(v_o)^0/(v_o)^I = 1 + [(1 + 1/K_I^*)/(1 + 1/K_M^*)][X_I/(1 - X_I)] \quad (3)$$

where X_I is the mole fraction of the inhibitor and K_I* is the dissociation constant of the inhibitor determined from the previous section. As shown in Table V, the mole fraction of MJ33 required for 50% inhibition for the hydrolysis of $DC_{14}PM$ is clearly larger for Y52V relative to WT, and the K_M* values calculated from such experiments are 0.65 and >3.5 for WT and Y52V, respectively. The value given for Y52V is only a lower limit because the concentration of ligands at the interface of the neutral diluent can be manipulated only in a limited range of the mole fraction, typically <0.3. Nonetheless, *the higher K_M* value agrees well with the higher K_S*, K_P*, and K_I* values for Y52V* (relative to WT) reported in the previous section.

(*b*) *$N_S k_i$, the Apparent Second-Order Rate Constant.* As explained by Berg et al. (1991), N_S is the number of substrate molecules hydrolyzed by each enzyme molecule when there is at most one enzyme molecule per enzyme-containing vesicle, and k_i is the relaxation time (first-order relaxation constant) of this process. Since the number of substrate molecules hydrolyzed by each enzyme molecule should be the same as the number of substrate molecules on the outer layer of a vesicle, which is a fixed number, N_S is actually an indicator of the functionally active enzyme molecules. For all the mutants reported in this paper, the values of N_S are constant within a 10% range (data not shown), which suggests that all mutant enzymes are functional and bind to $DC_{14}PM$ vesicles with such a high affinity that there is no noticeable intervesicle exchange. According to Berg et al. (1991), the product $N_S k_i$ can be considered as the second-order rate constant k_{cat}/K_m in Michaelis–Menten kinetics but is described by the following equation in the scooting mode:

$$N_S k_i = k_{cat}/[K_M^*(1 + 1/K_P^*)] \quad (4)$$

The $N_S k_i$ values for WT, Y52V, and Y73S are 30, 2.5, and 7.5 s^{-1}, respectively.

(*c*) *Other Derived Parameters.* The ratio k_{cat}/K_M* can be derived from eq 4. For WT PLA2, $N_S k_i = 30\ s^{-1}$ and $K_P^* = 0.03$, which give $k_{cat}/K_M^* = 1030\ s^{-1}$; For the Y52V mutant, $N_S k_i = 2.5\ s^{-1}$ and $K_P^* = 0.25$, which give $k_{cat}/K_M^* = 12.5\ s^{-1}$. Since the K_M* values are 0.65 and >3.5 for WT and Y52V, respectively, the k_{cat} values should be 670 and >50 s^{-1}, respectively. Alternatively, the k_{cat} values can be calculated from eq 1 using the measured v_o and K_M* values under the condition $X_S = 1$; the k_{cat} values thus obtained are 545 and >50 s^{-1} for WT and Y52V, respectively. These analyses suggest that the theoretical k_{cat} value (turnover number under saturating conditions) of Y52V is lower than that of WT by <10-fold. If it is assumed that the K_M* value also increases by 10-fold for Y52V (the same increase as equilibrium dissociation constants), the k_{cat} value of Y52V should be 80. Thus, *the kinetic behavior of Y52V is characterized by a 30-fold decrease in the v_o value, a ca. 10-fold decrease in the affinity of E* toward substrates and inhibitors, a ca. 5–10-fold decrease in k_{cat}, and a ca. 80-fold decrease in k_{cat}/K_M*.*

Discussion

The preceding sections present rigorous analyses of the structural and functional roles of the highly conserved active site residues Tyr-52 and Tyr-73. The results indicate that the H-bonding between these two tyrosines and Asp-99 is nonessential to catalysis, but replacement of Tyr-52 with valine (and other nonaromatic residues) lowers the affinities of the enzyme toward substrates, products, and inhibitors by ca. 10-fold and also causes a decrease in k_{cat} by 5–10-fold. Tyr-73 clearly plays important structural roles; whether it also plays a functional role similar to that of Tyr-52 is uncertain. The broader implications of our results are discussed in the followed sections.

Binding of the Enzyme to the Interface. The mutation of residues 52 and 73 did not noticeably influence the E to E* equilibrium as monitored by the kinetic and direct binding experiments. The fact that the E* to E*S step, but not the E to E* step, was perturbed in Y52V provides strong support to the previous suggestion (Ramiraz & Jain, 1991; Berg et al., 1991; Jain et al., 1991a,b) that these two steps are completely independent. The results in Figure 11 clearly show that the changes in A_{292} are caused by the E*I form but not the E* form. These results should have a far-reaching impact on the field, since these two forms were not distinguished in most spectroscopic (Kuipers et al., 1991; Dekker et al., 1991b) and calorimetric (Biltonen et al., 1991) studies. Since the alkylphosphocholine often used in these studies for converting E to E* actually also binds to the active site (Jain et al., 1991d), the E* species in these reports is actually a mixture of E* and E*I.

Comparison between Micellar and Scooting Mode Assay Systems. Interestingly, all five assay systems in Table I gave qualitatively similar results in the overall rates: the activities of Phe mutants are comparable to the activity of WT, while the activities of nonaromatic mutants decrease substantially. However, quantitatively the extents of decrease are greatest for DC_8PC micelles (130–750-fold) and smallest for DC_8PM micelles (<10-fold). The large variation in these results points to the importance of understanding the real meaning of each assay system in properly interpreting the structure–function relationship of PLA2 and other enzymes involved in interfacial catalysis.

The $DC_{14}PM$ vesicle system offers a clear advantage in permitting detailed analysis of the perturbations of specific steps in the scooting mode. The results indicate a ca. 10-fold decrease in the affinity of Y52V at the interface (i.e., the E* form) for substrates, products, and inhibitors at the interface, and a <10-fold decrease in k_{cat}. The catalytic activity at the interface, k_{cat}/K_M*, is lowered by 85-fold for Y52V.

What factors might contribute to the larger "dynamic range" in the $k_{cat,app}$ of the DC_8PC micelles? *There are two separate issues here: what $k_{cat,app}$ and $K_{m,app}$ actually measure, and why the decreases in the k_{cat} are so large for DC_8PC.* Regarding the first issue, the $K_{m,app}$ of micelles reflects affinity of the enzyme to micelles (similar to the E to E* step in the scooting mode). The relatively small perturbation in the $K_{m,app}$ of Y52V is consistent with the lack of perturbation in the E to E* step in the scooting mode. However, even if the $K_{m,app}$ values were very different, they should not be responsible for the differences in $k_{cat,app}$ since the latter was determined when all enzyme molecules are bound to micelles. The $k_{cat,app}$ of micelles can at best be compared with the v_o of the scooting mode since even when all enzyme molecules are associated with micelles, the active site may not be saturated (the actual mole fraction of substrate cannot exceed 1). In reality, $k_{cat,app}$ could be further limited by the exchange of substrate as well as enzyme molecules between different micelles (Berg et al., 1991; Jain et al., 1991c); but this factor should result in a smaller instead of a larger dynamic range for micelles since it would have a smaller effect on the mutants with slower overall rates of hydrolysis. This could account for the observation that the dynamic range of the activities of DC_8PM micelles is smaller than that of the v_o of $DC_{14}PM$ vesicles, as shown in Table I.

The large dynamic range for DC_8PC micelles relative to DC_8PM micelles (the second issue) is apparently a "substrate specificity" effect, i.e., PC is a poorer substrate than PM for the mutants while they are equally good substrates for the WT PLA2. The specific step(s) responsible for such a change in substrate specificity is not clear since it is not yet possible to deduce microscopic rate and equilibrium constants for PC micelles for or PC vesicles. However, since the main perturbation in Y52V is in binding of a substrate molecule to the active site, it is conceivable that this perturbation could be larger for PC than for PM (as further elaborated from structural point of view later in the next section). The larger perturbation in the active site interactions with PC could lead to worse $k_{cat,app}$ for PC micelles by raising the "K_m" (the E* to E*S step in terms of interfacial catalysis), by lowering the effective surface concentration below mole fraction 1, and/or by lowering the rates of other steps, including the chemical step.

Roles of Tyr-52 and Tyr-73 in Supporting Activity. The hydrogen bonds between the phenolic hydroxyl groups of both Tyr-52 and Tyr-73 and the carboxylate of Asp-99 are clearly nonessential to catalysis by PLA2. However, upon further loss of either of the aromatic rings at positions 52 and 73 through aliphatic substitutions, the activity of the enzyme is significantly diminished. Detailed kinetic and equilibrium analyses of Y52V indicate that the perturbation lies primarily in k_{cat}/K_M*. Since neither proton NMR nor conformational stability have been perturbed significantly, the perturbations in the kinetic behavior of Y52V are not caused by global conformational changes.

The question, then, is how to explain the perturbation in the function of Y52V in terms of enzyme–substrate interactions at the active site. Perturbation of direct interactions with the substrate, specifically the methylenes of the choline headgroup, are possible on the basis of crystal structures of enzyme–inhibitor complexes (Noel et al., 1991; White et al., 1990; Thunnissen et al., 1989). Such a perturbation should be less significant for the methanol headgroup, and thus could very well explain the large dynamic range in the $k_{cat,app}$ of DC_8PC micelles versus the small dynamic range for DC_8PM micelles (i.e., the change in the substrate specificity of Y52V) as noted in the previous section. Another possible interpretation is that local structural changes produced by aliphatic substitutions at position 52 affect the orientation of other critical residues (e.g., Tyr-69 or others). A third possibility is that Tyr-52, along with the extensive network of conserved aromatic side chains at or near the active site (including Phe-5, -22, -106 and Tyr-52, -69, -73, -75), provides a unique hydrophobic, aromatic environment that somehow augments catalysis.

Structure–Function Relationships of Tyr-52 and Tyr-73 in the Hydrogen-Bonding Network. Speculation regarding the importance of the integrity of the hydrogen-bonding network to PLA2 activity has persisted for some time. Prior to our report, it seemed quite plausible to hypothesize that the contributions of the absolutely conserved phenolic hydroxyls Tyr-52 and Tyr-73 to this network were critical to activity toward aggregated substrates. Our results demonstrate that this is not the case. However, kinetic results alone do not suggest any alternative structure–function relationships for these phenolic hydroxyls. Such networks in other enzymes, however, have been implicated in contributing to stability (Gruetter et al., 1987). This prompted us to pursue the possible contributions of these residues (through the hydrogen bonding network) to conformational stability. Interestingly, removal of the Tyr-73 phenolic hydroxyl by mutating to Phe, Ala, Ser, or Lys lowered the $\Delta G_d^{H_2O}$ by 4–5 kcal/mol. These changes are among the largest ever reported for site-directed mutants of proteins (Shortle, 1989; Shortle et al., 1990) and to our knowledge the largest among active site mutants. The contribution of the hydroxyl of Tyr-52 appears to be less critical.

Close inspection of the crystal structure of bovine pancreatic PLA2 (Dijkstra et al., 1981a,b; Noel et al., 1991) revealed that Tyr-52, Tyr-73, and Asp-99 are located in the C-helix, the β-wing, and the E-helix, respectively (see Figure 2). The C-helix and the E-helix are also held together by two disulfide bonds (C51/C98 and C44/C105) other than the H-bond between Tyr-52···Asp-99. The modest $\Delta\Delta G_d^{H_2O}$ values for Tyr-52 mutants can be explained in this manner. On the other hand, according to the crystal structure of WT PLA2, the Tyr-73···Asp-99 H-bonding appears to be the only stabilizing force between the E-helix and the unanchored β-segment 74–78. This could explain the large $\Delta\Delta G_d^{H_2O}$ values seen for mutations eliminating the Tyr-73 phenolic hydroxyl. Apparently, the unique positioning of the H-bonding hydroxyl afforded by the phenyl ring is required since substitution to Lys or Ser did not restore the loss of stability. Indeed, such structure–function relationships for residues participating in hydrogen-bonding networks have been previously reported (Gruetter et al., 1987). There are also a number of examples in which aromatic residues serve to connect secondary structure elements (Nockolds et al., 1972; Moews & Kretsinger, 1975). PLA2 structure appears to utilize an elegant combination of both stabilizing features.

Roles of Aromatic–Aromatic Pairs in the Conformational Stability of PLA2. The conformational stability of the porcine enzyme is reported to be near 7 kcal/mol (Pickersgill et al., 1991). Our results for the highly homologous bovine enzyme are in agreement with this result. Both of these values put PLA2 among the most stable of enzymes (Pace, 1990). This is consistent with the many references in the literature to the remarkable resilience of this enzyme under many otherwise denaturing conditions.

However, the contributions of the aromatic rings of Tyr-52 and Tyr-73 to the conformational stability of PLA2 appear

to be in contrast to reports of this type for other enzymes. Examination of the wild-type crystal structure of PLA2 reveals that Tyr-52 and Tyr-73 each participates in edge-to-face, T-shaped, aromatic–aromatic interactions with Tyr-69 and Tyr-75, respectively (Figure 2). There is some theoretical and experimental evidence that suggests such arrangements are energetically favorable and contribute to protein conformational stability (Burley & Petsko, 1985; Serrano et al., 1991). For PLA2, substitution of Tyr-73 by Phe resulted in a large decrease in conformational stability, yet no further loss of stability was observed upon substitution of the ring for aliphatic side chains. Apparently, maintenance of hydrogen-bonding ability of Tyr-73 is more critical to $\Delta G_d^{H_2O}$ than aromatic–aromatic interactions between Tyr-73 and Tyr-75. Loss of aromaticity and hydrogen-bonding capability at position 52 also perturbs $\Delta G_d^{H_2O}$ relatively little. These results warrant further study of the contributions of aromatic residues to conformational stability of proteins.

Structure, Function, and Stability Relationships in PLA2. The results of this work demonstrate that the relationships between structure, function, and conformational stability of proteins are less straightforward than we like to believe. From the viewpoints of sequence homology, structural conservation, and molecular evolution, one would tend to predict that the H-bonds between Asp-99 and the two tyrosine residues are important in function; apparently, this is not the case. Instead, it was the disruption of the aromatic rings that led to significant changes in catalytic activity. One would then predict that such changes are probably caused by structural perturbations (Dupureur et al., 1990). However, proton NMR analysis suggests that the conformation of Y52V is little perturbed. For Tyr-73, removal of the tyrosyl hydroxyl group resulted in unexpectedly little effect on activity but a remarkably large effect on $\Delta G_d^{H_2O}$. Interestingly, further removal of the aromaticity caused large decreases in the activity but did not further perturb the conformational stability. Thus, although we have been able to analyze both functional and structural properties of the mutant enzymes in detail and have gained considerable insight into structure–function relationships for these tyrosines, we must await further exploration of the active site before these interrelationships can be fully understood.

After submission of this paper, we observed that the conformational flexibility in Y73A also occurred in Y73S and D99N and perceived that such a behavior is characteristic of (although not identical to) the "molten globule", a protein conformational state characterized by great flexibility with retention of secondary structures (Baum et al., 1989; Ptitsyn & Semisotnov, 1991; Fink et al., 1991). The results and interpretation to this end have been described in a preliminary communication (Dupureur et al., 1992).

Acknowledgments

We are indebted to Xiaoyan Zhang for purifying some of the mutant enzymes.

References

Achari, A., Scott, D., Barlow, P., Vidal, J. C., Otwinowski, Z., Brunie, S., & Sigler, P. (1987) *Cold Spring Harbor Symp. Quant. Biol. 52*, 441–452.

Atkins, G. L., & Nimmo, I. A. (1975) *Biochem. J. 149*, 775–779.

Baum, J., Dobson, C. M., Evans, P. A., & Hanley, C. (1989) *Biochemistry 28*, 7–13.

Berg, O. G.,Yu, B.-Z., Rogers, J., & Jain, M. K. (1991) *Biochemistry 30*, 7283–7297.

Biltonen, R. L., Lathrop, B. K., & Bell, J. D. (1991) *Methods Enzymol. 197*, 234–248.

Brockerhoff, H. (1968) *Biochim. Biophys. Acta 159*, 296–303.

Brunie, S., Brolin, J., Gewirth, D., & Sigler, P. B. (1985) *J. Biol. Chem. 260*, 9742–9749.

Burley, S. K., & Petsko, G. A. (1985) *Science 229*, 23–28.

Dekker, N., Peters, A. R., Slotboom, A. J., Boelens, R., Kaptein, R., & de Haas, G. H. (1991a) *Biochemistry 30*, 3135–3147.

Dekker, N., Peters, A. R. Slotboom, A. J., Kaptein, R., Dijkman, R., & de Haas, G. H. (1991b) *Eur. J. Biochem. 199*, 601–607.

Deng, T., Noel, J. P., & Tsai, M.-D. (1990) *Gene 93*, 229–234.

Dijkstra, B. W., Drenth, J., Kalk, K. H., & Vandermaelen, P. J. (1978) *J. Mol. Biol. 124*, 53–60.

Dijkstra, B. W., Drenth, J., & Kalk, K. H. (1981a) *Nature 289*, 604–606.

Dijkstra, B. W., Kalk, K. H., Hol, W. G. J., & Drenth, J. (1981b) *J. Mol. Biol. 147*, 97–123.

Dijkstra, B. W., Renetseder, R., Kalk, K. H., Hol, W. G. J., & Drenth, J. (1983) *J. Mol. Biol. 168*, 163–179.

Dijkstra, B. W., Kalk, K. H., Drenth, J., de Haas, G. H., Egmond, M. R., & Slotboom, A. J. (1984) *Biochemistry 23*, 2759–2766.

Dufton, M. J., Eaker, D., & Hider, R. C. (1983) *Eur. J. Biochem. 137*, 537–544.

Dupureur, C. M., Deng, T., Kwak, J.-G., Noel, J. P., & Tsai, M.-D. (1990) *J. Am. Chem. Soc. 112*, 7074–7076.

Dupureur, C. M., Li, Y., & Tsai, M.-D. (1992) *J. Am. Chem. Soc. 114*, 2748–2749.

Fink, A. L., Calciano, L. J., Goto, Y., & Palleros, D. (1991) in *Conformations and Forces in Protein Folding* (Nall, B. T., & Dill, K. A., Eds.) pp 169–174, American Association for the Advancement of Science, Washington, DC.

Fisher, J., Primrose, W. U., Roberts, G. C. K., Dekker, N., Boelens, R., Kaptein, R., & Slotboom, A. J. (1989) *Biochemistry 28*, 5939–5946.

Greenfield, N., & Fasman, G. D. (1969) *Biochemistry 8*, 4108–4116.

Gruetter, M. G., Gray, T. M., Weaver, L. H., Alber, T., Wilson, K., & Matthews, B. W. (1987) *J. Mol. Biol. 197*, 315–329.

Hille, J. D. R., Egmond, M. R., Dijkman, R., Van Oort, M. G., Jirgensons, B., & de Haas, G. H. (1983) *Biochemistry 22*, 5347–5353.

Jain, M. K., & Vaz, W. L. C. (1987) *Biochim. Biophys. Acta 906*, 1–8.

Jain, M. K., & Berg, O. G. (1989) *Biochim. Biophys. Acta 1002*, 127–156.

Jain, M. K., & Rogers, J. (1989) *Biochim. Biophys. Acta 1003*, 91–97.

Jain, M. K., & Gelb, M. H. (1991) *Methods Enzymol. 197*, 112–125.

Jain, M. K., Egmond, M. R., Verheij, H. M., Apitz-castro, R. J., Kijkman, R., & de Haas, G. H. (1982) *Biochim. Biophys. Acta 688*, 341–348.

Jain, M. K., Rogers, J., Jahagirdar, D. V., Marecek, J. F., & Ramirez, F. (1986) *Biochim. Biophys. Acta 860*, 435–447.

Jain, M. K., Yu, B.-Z., Rogers, J., Ranadive, G. N., & Berg, O. G. (1991a) *Biochemistry 30*, 7306–7317.

Jain, M. K., Ranadive, G. N., Yu, B.-Z., & Verheij, H. M. (1991b) *Biochemistry 30*, 7330–7340.

Jain, M. K., Rogers, J., Berg, O., & Gelb, M. H. (1991c) *Biochemistry 30*, 7340-7348.

Jain, M. K., Tao, W., Rogers, J. Arenson, C., Eibl, H., & Yu, B. Z. (1991d) *Biochemistry 30*, 10256–10268.

Kuipers, O. P., Franken, P. A., Hendriks, R., Verheij, H. M., & de Haas, G. M. (1990) *Protein Eng. 4*, 199-204.

Kuipers, O. P., Vincent, M., Brochon, J.-C., Verheij, H. M., de Haas, G. H., & Gallay, J. (1991) *Biochemistry 30*, 8771–8775.

Maraganore, J. M., Poorman, R. A., & Heinrikson, R. L. (1987) *J. Protein Chem. 6*, 173–189.

Meyer, H., Herhoef, H., Hendriks, F. F. A., Slotboom, A. J., & de Haas, G. H. (1979) *Biochemistry 18*, 3582–3588.

Moews, P. C., & Kretsinger, R. H. (1975) *J. Mol. Biol. 91*, 201–228.

Nieuwenhuizen, W., Kunze, H., & de Haas, G. H. (1974) *Methods Enzymol. 32B*, 147–154.

Nockolds, C. E., Kretsinger, R. H., Coffee, C. J., & Bradshaw, R. A. (1972) *Proc. Natl. Acad. Sci. U.S.A. 69*, 581–584.

Noel, J. P., Bingman, C. A., Deng, T., Dupureur, C. M., Hamilton, K. J., Jiang, R.-T., Kwak, J.-G., Sekharudu, C., Sundaralingam, M., & Tsai, M.-D. (1991) *Biochemistry 30*, 11801–11811.

Nozaki, Y. (1972) *Methods Enzymol. 26*, 43–50.

Pace, C. N. (1975) *Crit. Rev. Biochem. 3*, 1–43.

Pace, C. N. (1990) *Trends Biochem. Sci. 15*, 1–4.

Pace, C. N. (1986) *Methods Enzymol. 131*, 266–279.

Pace, C. N., & Marshall, H. F. (1980) *Arch. Biochem. Biophys. 199*, 270–276.

Pickersgill, R. W., Sumner, I. G., Collins, M. E., Warwicker, J., Perry, B., Bhat, K. M., & Goodenough, P. W. (1991) *FEBS Lett. 281*, 219–222.

Ptitsyn, O. B., & Semisotnov, G. V. (1991) in *Conformations and Forces in Protein Folding* (Nall, B. T. & Dill, K. A., Eds.) pp 155–168, American Association for the Advancement of Science, Washington, DC.

Radvanyi, F., Jordan, L., Russo-Marie, F., & Bon, C. (1989) *Anal. Biochem. 177*, 103–109.

Ramiraz, F., & Jain, M. K. (1991) *Proteins: Struct., Funct., Genet. 9*, 229–239.

Renetseder, R., Brunie, S., Dijkstra, B. W., Drenth, J., & Sigler, P. B. (1985) *J. Biol. Chem. 260*, 11627–11634.

Scanu, A. M., van Deenen, L. L. M., & de Haas, G. H. (1969) *Biochim. Biophys. Acta 181*, 471–473.

Scott, D. L., Otwinowski, Z., Gelb, M. H., & Sigler, P. B. (1990) *Science 250*, 1563–1567.

Serrano, L., Bycroft, M., & Fersht, A. R. (1991) *J. Mol. Biol. 218*, 465–475.

Shortle, D. (1989) *J. Biol. Chem. 264*, 5315–5318.

Thunnissen, M. M. G. M., AB, E., Kalk, K. H., Drenth, J., Dijkstra, B. W., Kuipers, O. P., Dijkman, R., de Haas, G. H., & Verheij, H. M. (1990) *Nature 347*, 689–691.

van Dam-Mieras, M. C. E., Slotboom, A. J., Pieterson, W. A., & de Haas, G. H. (1975) *Biochemistry 14*, 5387–5394.

van den Bergh, C. J., Bekkers, A. C. A. P. A., de Geus, P., Verheij, H. M., & de Haas, G. H. (1987) *Eur. J. Biochem. 170*, 241–246.

van Scharrenburg, G. J. M., Puijk, W. C., Egmond, M. R., van der Schaft, P. H., de Haas, G. H., & Slotboom, A. J. (1982) *Biochemistry 21*, 1345–1352.

van Scharrenburg, G. J. M., Slotboom, A. J., de Haas, G. H., Mulqueen, P., Breen, P. J., & Horrocks, W. DeW., Jr. (1985) *Biochemistry 24*, 334–339.

Verheij, H. M., Slotboom, A. J., & de Haas, G. H. (1981) *Rev. Physiol. Biochem. Pharmacol. 91*, 91–227.

Volwerk, J. J., & de Haas, G. H. (1982) *Lipid–Protein Interact. 1*, 69–149.

Waite, M. (1978) *The Phospholipases*, Plenum Press, New York.

White, S. P., Scott, D. L., Otwinowski, Z., Gelb, M. H., & Sigler, P. (1990) *Science 250*, 1560–1563.